



# Monte Carlo study of patient and medical staff radiation exposures during interventional cardiology

M. Bhar, S. Mora, O. Kadri, S. Zein, K. Manai, S. Incerti

## ► To cite this version:

M. Bhar, S. Mora, O. Kadri, S. Zein, K. Manai, et al.. Monte Carlo study of patient and medical staff radiation exposures during interventional cardiology. *Physica Medica*, 2021, 82, pp.200-210. 10.1016/j.ejmp.2021.01.065 . hal-03154283

**HAL Id: hal-03154283**

**<https://hal.science/hal-03154283>**

Submitted on 2 Mar 2021

**HAL** is a multi-disciplinary open access archive for the deposit and dissemination of scientific research documents, whether they are published or not. The documents may come from teaching and research institutions in France or abroad, or from public or private research centers.

L'archive ouverte pluridisciplinaire **HAL**, est destinée au dépôt et à la diffusion de documents scientifiques de niveau recherche, publiés ou non, émanant des établissements d'enseignement et de recherche français ou étrangers, des laboratoires publics ou privés.

# Monte Carlo study of patient and medical staff radiation exposures during interventional cardiology

M. Bhar<sup>a,b</sup>, S. Mora<sup>c</sup>, O. Kadri<sup>b</sup>, K. Manai<sup>b</sup>, S. Zein<sup>d</sup> and S. Incerti<sup>d</sup>

<sup>a</sup>*Higher Institute of Medical Technologies of Tunis, Tunis El Manar University, Tunisia*

<sup>b</sup>*Nuclear Physics and High Energy Unit, Faculty of Sciences of Tunis, Tunis El Manar University, Tunisia*

<sup>c</sup>*University Hospital Center of Bordeaux. Bordeaux, France*

<sup>d</sup>*Université de Bordeaux, CNRS/IN2P3, UMR5797, Centre d'Études Nucléaires de Bordeaux Gradignan, 33175 Gradignan, France*

---

## Abstract

The aim of this study is to assess the radiation exposure of the patient and the medical staff during interventional cardiology procedures. Realistic exposure scenarios were developed using the adult reference anthropomorphic phantoms adopted by the International Commission on Radiological Protection (*ICRP110<sub>Male</sub>* and *ICRP110<sub>Female</sub>*), and the radiation transport code GEANT4 (version 10.3). The calculated equivalent and effective doses were normalised by the simulated Kerma-Area Product (KAP), resulting in two conversion coefficients  $H_T/KAP$  and  $E/KAP$ . To properly evaluate the risk of exposure, several dose-dependent parameters have been investigated, namely: radiological parameters (tube kilovoltage peak (kVp), type of projection, field size (FOV)), and operator positions. Four projections (*AP*, *PA*, *LAO25°* and *RAO25°*) were simulated for three X-ray energy spectra (80, 100 and 120 kVp) with four different values of FOV ( $15 \times 15 \text{ cm}^2$ ,  $20 \times 20 \text{ cm}^2$ ,  $25 \times 25 \text{ cm}^2$  and  $30 \times 30 \text{ cm}^2$ ). The results showed that the conversion coefficients values increase with increasing tube voltage as well as the FOV size. Recommended projection during the interventional cardiology procedures, whenever possible, should be the *PA* projection rather than *AP* projection. The most critical projection for the patient and the main operator is the *RAO25°* projection and the *LAO25°* projection respectively. The comparison of our results with the literature data showed good agreement allowing their use in the dosimetric characterization of interventional cardiology procedures.

*Key words:* Interventional cardiology, numerical human phantom, effective dose, equivalent dose, GEANT4 code.

---

## 1 Introduction

Interventional cardiology (IC) performed under the control and guidance of an X-ray imaging tool is a widespread technique used for diagnosis and treatment of various cardiac pathologies. However, during this procedure, the patient and the medical staff are exposed to significant radiation doses. In general, the received doses in IC are much higher than other radiological procedures, including in nuclear medicine [1].

Given their complexity, the long duration of IC procedures in addition to the required proximity of operators to the patient who represents the primary source of scattered radiation result in considerable dose.

In this regard, special evaluation of the exposure of the patient and the medical staff is necessary in order to ensure their protection. The direct evaluation of the absorbed dose to an organ or a tissue remains a difficult and impractical task, requiring, in general, delicate and invasive procedure. Therefore, Monte Carlo (MC) simulation is considered as an effective tool to simulate the interaction of particles with matter and to estimate the organ doses for computational anthropomorphic human phantoms [2–6].

Modeling of the human’s anatomy has developed significantly over the last decades, moving towards more realism and personalization. Nowadays, there are mainly three morphometric categories (reference, patient-dependent and patient-specific), as well as three phantom format types (stylized, voxel and hybrid). Here, specific emphasis is given to voxel type and reference category using the ICRP reference male and female voxellized phantoms.

Simulation codes such as MCNP[7, 8], PENELOPE[9], EGSnrc[10], FLUKA[11], GEANT4 [12–15] and its derivative GATE[16], provide the tools for calculating radiation doses and are commonly used in several studies focusing on patient and staff protection in interventional scenarios [2–6]. Nevertheless, to the best of our knowledge, there are no studies that assess radiation exposure in IC procedures using the *ICRP110* voxellized phantoms [17] and GEANT4 toolkit.

The dosimetric assessment for the patient and the medical staff is crucial and it is possible to take advantage of these highly sophisticated tools to determine the absorbed doses in a very accurate way. Therefore, GEANT4 and the *ICRP110* phantoms have been employed in this study to determine

---

*Email address:* `bhar.maroua@yahoo.com` (M. Bhar).

the equivalent and effective doses normalised by the Kerma-Area Product (KAP) ( $H_T/KAP$  and  $E/KAP$ ) for patient and medical staff during cardiac intervention procedures and considering the influence of several factors: the energy spectra of the X-ray tube, the size of the field, the type of irradiation projection, and also the position of the operator against the X-ray source.

First, an overall study of radiation exposure dependent parameters for both the patient and the medical staff is performed. The next part was to validate our findings in comparison with published studies. The efficiency of the innovative radiation protection equipment: mobile radiation protection cabin (RPC), against routine protection equipment is then investigated in the last part.

## 2 Material and Methods

### 2.1 Computational human phantom simulation

GEANT4 (GEometry ANd Tracking) is a toolkit for the simulation of particles transport through matter. This code is a set of C++ classes that can be used to design a simulation application [18, 19]. Its areas of application include high energy, nuclear and accelerator physics, as well as studies in medical and space science etc. [20]. Different parameters can be set up to better simulate the radiation transport and, in this work photoelectric-effect, Compton and Rayleigh scattering for photons, Bremsstrahlung, and multiple scattering models for electrons have been selected.

The values of 1 *keV* and 10 *keV* are set respectively as the energy thresholds for photons and electrons. During all simulations, the standard electromagnetic physics options were used which are governed by the specific physics builder "G4EmStandardPhysics" to achieve our purposes.

To model the patient and the medical staff, we used the reference male and female phantoms that are adopted by the *ICRP110*. Their design is based on tomographic images of a real man and a real woman. Their main characteristics are described in table 1. A more detailed description is included in the ICRP publication 110 [17].

To manage the large number of voxels representing the phantoms, we used the nested parameterisation approach provided by the *G4VNestedParameterisation* class [21]. This specific class was also introduced in the duplication of the phantom to model a patient and the medical staff in the same exposure procedure.

Property	Male	Female
Height (m)	1.76	1.63
Weight (kg)	73	60
Number of voxels	1,946,375	3,886,202
Slice thickness (mm)	8	4.84
Pixel size ( $mm^2$ )	$(2.137)^2$	$(1.775)^2$
Voxel volume ( $mm^3$ )	36.54	15.25
Number of columns	254	299
Number of rows	127	137
Number of slices	220	346

Table 1

Main characteristics of  $ICRP110_{Male}$  and  $ICRP110_{Female}$  reference phantoms

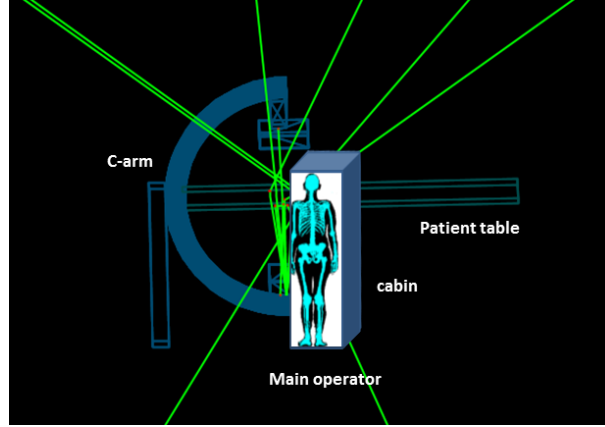


Figure 1. Simulated setup including C-arm equipment, patient's table, ICRP110 phantom representing the main operator and radiation protection cabin. Some tracks were visualized using the HepRapp visualization tool [22].

## 2.2 Description of the simulated scenarios

In all the scenarios described below, a cardiac intervention room of the University Hospital Center of Bordeaux, France, was modelled. The walls of the room are made of concrete or plaster covered with lead. A patient table made of carbon fibre ( $\rho = 1.25 \text{ g/cm}^3$ ) with a thickness of  $33 \text{ mm}$  has been placed at a height of  $109.85 \text{ cm}$  from the floor.

In this space, the main components of the X-ray equipment were inserted in addition to the patient and the operators. The X-ray tube has been simplified to a point source emitting a conical beam of photons. As shown in Figure 1, the simulated C-arm machine supports at its two extremities the X-ray tube with  $11.35 \text{ g/cm}^3$  density lead shield and the CsI imaging device with a

density of  $1.25 \text{ g/cm}^3$  (a box representing the image detector :  $50 \times 50 \times 13 \text{ cm}^3$ ) with an inner diameter of about  $1 \text{ m}$ . The source-skin distance was set at approximately  $61.5 \text{ cm}$ . These distances have been maintained constant for all exposure conditions and are roughly representative of real practice.

For a realistic modeling of the X-ray spectrum following the recommendations, we used the *SpekCalc* software [23]. Several radiographic parameters of choice (kVp, filtrations, anode angle ...) can be introduced. The generated spectra were later included in the GEANT4 code.

Three energy (and Half-Value Layer) spectra were studied:  $80 \text{ kVp}$  (HVL=  $3.2 \text{ mm Al}$ ),  $100 \text{ kVp}$  (HVL=  $3.8 \text{ mm Al}$ ) and  $120 \text{ kVp}$  (HVL=  $4.3 \text{ mm Al}$ ). A shaping filter was introduced at the output of the primary beam, in order to reproduce the square shape of the field and focalise it on the examined region. The role of this filter is to stop all photons outside of its central square orifice. Four different values of field size (designed by FOV: Field Of View) were studied:  $15 \times 15 \text{ cm}^2$ ,  $20 \times 20 \text{ cm}^2$ ,  $25 \times 25 \text{ cm}^2$  and  $30 \times 30 \text{ cm}^2$ .

Four simulated beam projections were simulated: antero-posterior (AP), postero-anterior (PA), Left Anterior Oblique ( $LAO25^\circ$ ), and Right Anterior Oblique ( $RAO25^\circ$ ). In all cases, the beam of photons is focused on the patient's heart, to mimic an interventional cardiology procedure (Figure 2).

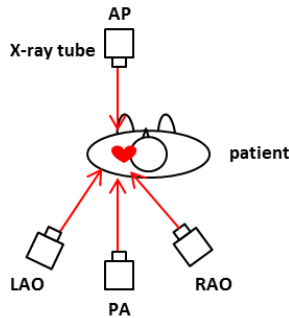


Figure 2. Schematic sketch of the studied projection modalities: antero-posterior (AP), postero-anterior (PA), Left Anterior Oblique ( $LAO25^\circ$ ), and Right Anterior Oblique ( $RAO25^\circ$ ).

Basically we will have five different scenarios to explore, acting on the cited exposure-dependent parameters (see Table 2). It is very important to note that in a given scenario of this study, the intervention scene contains at least two exposed members. Therefore at least one duplication of the phantom was made, and the duplication is done by keeping always the same type of phantom ( $ICRP110_{Male}$  /  $ICRP110_{Female}$ ). In other words, during a given scenario, the included members are all male or all female.

- Scenario 1: Three male exposed members: a patient (lying on the surgical

Protection equipment	Scenarios number	Simulated person	phantom used	Peak volt-age (kVp)	FOV ( $cm^2$ )	Projection modality
routine equipment	1	patient two opera-tors	$ICRP110_{Male}$	80/100/120	15/20/25/30	PA
	2	patient ten opera-tors	$ICRP110_{Male}$	80/100/120	20	PA
	3	patient one operator	$ICRP110_{Male}$	100	20/30	AP/PA/LAO25°/RAO25°
	4	4.1 patient one operator 4.2 patient one operator	$ICRP110_{Male}$ $ICRP110_{Female}$	80/100/120	20/30	PA/LAO25°/RAO25°
RPC	5	patient one operator	$ICRP110_{Male}$ $ICRP110_{Female}$	120	30	PA

Table 2

The five different scenarios explored in this study.

- table) and two professionals named as the main operator (located close to the right abdominal part of the patient) and the assistant operator (placed on the right side of the main operator). The calculation is performed for the PA projection by varying the kVp (80/100/120  $kVp$ ) or the FOV ( $15 \times 15 cm^2$  /  $20 \times 20 cm^2$  /  $25 \times 25 cm^2$  /  $30 \times 30 cm^2$ ) values. The conversion coefficients calculated are:  $E/KAP$  for the main/assistant male operators.
- Scenario 2: Eleven male exposed members: a patient and ten professionals. The medical staff are located approximately 35  $cm$  around the patient's table presenting the locations most likely to be occupied by personnel (as mentioned in literature [24] and shown in Figure 3). The distances from the X-ray beam isocenter are 54.1  $cm$ , for the first operator, 30.54  $cm$  for the second operator, 81.5  $cm$  for the third operator, 160.5  $cm$  for the fourth operator, 50.75  $cm$  for the fifth operator, 28  $cm$  for the sixth operator, 76.88  $cm$  for the seventh operator, 140.87  $cm$  for the eighth operator, 212.5  $cm$  for the ninth and 135.2  $cm$  for the tenth operator. The calculation is performed for the PA projection at a fixed value of the FOV ( $20 \times 20 cm^2$ ). The conversion coefficients calculated are:  $E/KAP$  for the ten male operators.
  - Scenario 3: Two male exposed members: the patient and the main operator. The calculation was made for the following beam qualities: at 100  $kVp$ ,  $20 \times 20 cm^2$  /  $30 \times 30 cm^2$  of the FOV and four modalities of projection : AP/PA/LAO25°/ RAO25°. The conversion coefficients calculated are: ( $E/KAP$  and  $H_T/KAP$ ) for the main male operator, and ( $E/KAP$  and

$H_T/KAP$ ) for the male patient.

- Scenario 4: Two sub-scenarios were tested using the male phantom first for both the patient and the operator (scenario 4.1) and then replacing them both with the female phantom (scenario 4.2). In both cases, the calculation was made for three beam projections:  $PA/LAO25^\circ/RAO25^\circ$  with the different values of kVp (80/100/120 kVp) and two values of FOV ( $20 \times 20 \text{ cm}^2/30 \times 30 \text{ cm}^2$ ). The conversion coefficients calculated are:  $E/KAP$  for the male/female patients.
- Scenario 5: Two male exposed members: the patient and the main operator. The calculation is performed for the PA projection with fixed values of the kVp (120 kVp) and FOV ( $30 \times 30 \text{ cm}^2$ ). The conversion coefficients calculated are:  $H_T/KAP$  for the male/female operators.

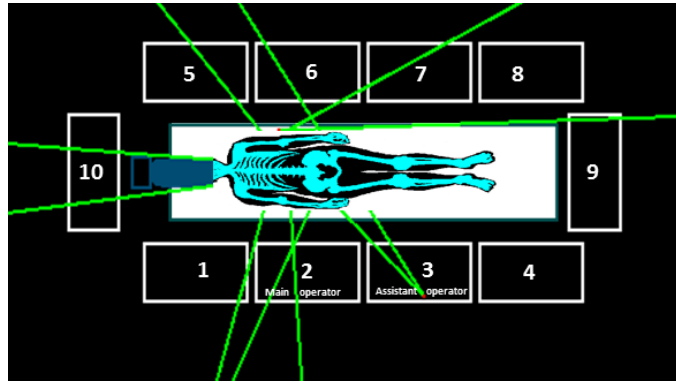


Figure 3. Possible positions occupied by the medical staff around the patient during an interventional procedure.

For each scenario, we tried to take into consideration several protective tools to make the radiation scenarios as close to reality as possible. In this sense, the protective equipment are modeled in two different ways:

- For 1<sup>st</sup>-4<sup>th</sup> scenarios: Routine equipment, a 0.5 mm thick protective lead apron, was modelled as a 0.5 mm thick lead box ( $x = 54.68 \text{ cm}$ ,  $y = 27.54 \text{ cm}$  and  $z = 120 \text{ cm}$ ), and placed around each worker extending from the thyroid level until the knees. Part of the lead box was cut to expose the shoulders and the arms of the operator. Protective eye glasses for the main operator were also modeled as a 0.35 mm thick lead layer. In addition to the personal protective shielding, 0.5 mm Pb shielding was reproduced for the ceiling and the walls, and sideways the patient table extending from table to floor.
- For 5<sup>th</sup> scenario: Radiation Protection Cabin (RPC). This device is modeled as a box of dimensions  $55.3 \times 50 \times 200 \text{ cm}^3$  to protect the main operator (see Figure 1). It is made of 2 mm thick lead glass (lead equivalent) where the practitioner can pass freely his arms through two holes in front of the patient to intervene.



### 2.3 Output data collection

The determination of the deposited energies ( $E_d$ ) in the *ICRP110* phantom organs/tissues was done with the specific scorer class *G4PSEnergyDeposit* with the exception of the red bone marrow (RBM) and the skeleton. The absorbed doses were then calculated by dividing the calculated deposited energy by the mass ( $m$ ) of the region of interest. Given that the radiation weighting factor ( $w_R$ ) of the photons is 1, the absorbed dose ( $Gy$ ) and the equivalent dose  $H_T(Sv)$  are numerically equivalent. The effective doses ( $E$ ) were determined by summing the products of equivalent doses with the tissue weighting factors ( $w_T$ ) recommended by the *ICRP103* using equation (1) [25]. When referring only to male models, the tissue weighting factors of the male model have been renormalized to one, the same have been done for the female model.

It is common to normalize the calculated equivalent and effective doses by another quantity, such as the Kerma-area Product (KAP ( $Gy.cm^2$ )), resulting in the two dosimetric quantities  $H_T/KAP$  and  $E/KAP$  studied in this work.

$$E/KAP = \sum_T w_T \left[ \frac{(H_T/KAP)_{Male} + (H_T/KAP)_{Female}}{2} \right] \quad (1)$$

where  $w_T$  is the organ/tissue weighting factor,  $(H_T/KAP)_{Male}$  is the calculated conversion factor for the *ICRP110<sub>Male</sub>* phantom and  $(H_T/KAP)_{Female}$  for the *ICRP110<sub>Female</sub>* phantom.

The KAP meter was designed as a simple parallelepiped filled with atmospheric air, and located between the source and the patient in the area perpendicular to the X-ray beam (15 *cm* from the focal point of the source). Its size has been modeled so that, its dimensions are compatible with the chosen field size. In each scenario, the simulated KAP value was used to normalize all the calculated dosimetric quantities.

The absorbed doses for RBM and bone surface were exceptionally calculated using the methodology described in ICRP Publication 116 [26]. The calculated values were then normalized by the KAP.

The hardware platform used to run the GEANT4 code (version 10.3) is a Linux (CentOS platform) Personal Workstation with 12 *GB* RAM and a 2.8 *GHz* CPU. The number of primary particles generated was 100 million attributing a low statistical uncertainty ( $<0.2\%$  for patient and  $<3\%$  for operators) for all irradiation scenarios, with simulation times varying from just under 3 hours to 8 hours.

### 3 Results and discussion

#### 3.1 Dosimetric evaluation for the exposed medical staff

In this section, the conversion coefficients  $E/KAP$  and  $H_T/KAP$  for the medical operator were studied as a function of different parameters influencing the dose.

##### 3.1.1 kVp effect

The values of  $E/KAP$  ( $\mu Sv/Gy.cm^2$ ) were calculated for the two professionals of the first scenario. Figure 4 shows that the  $E/KAP$  values increase with

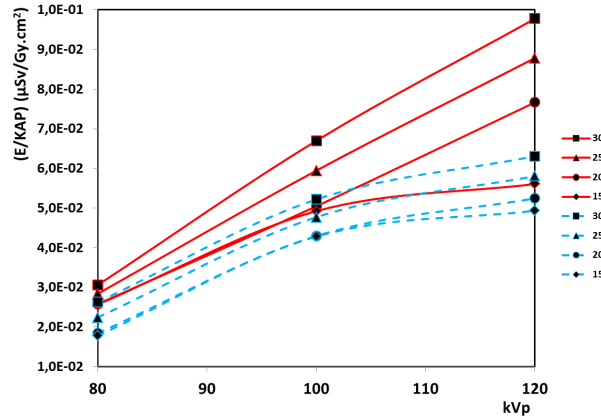


Figure 4. Occupational effective dose function of kVp for different FOV:  $15 \times 15 cm^2$  /  $20 \times 20 cm^2$  /  $25 \times 25 cm^2$  /  $30 \times 30 cm^2$  (continuous: main operator, discontinuous: assistant operator).

the increase of the tube voltage (varied from 80 to 120 kVp) regardless of the fixed FOV size ( $15 \times 15 cm^2$  /  $20 \times 20 cm^2$  /  $25 \times 25 cm^2$  /  $30 \times 30 cm^2$ ). This is due to the scattered radiation that is considered the main reason of exposure for the operators. The scattered radiation originates mainly from the patient's body that scatters the primary X-ray beam. By comparing the effective  $E/KAP$  doses received by the two operators, we notice that regardless of the field size, the primary operator always receives the highest doses due to their closest position relative to the primary radiation beam and the scattered radiation centre.

It must be kept in mind that the tube voltage has a significant effect on the occupational dose, hence the need for better optimization of this parameter.

### 3.1.2 FOV effect

According to Figure 4, the obtained results calculated for the first scenario exposure conditions show that an increase in the size of the FOV, from  $15 \times 15 \text{ cm}^2$  to  $30 \times 30 \text{ cm}^2$  at a given energy causes an increase in the effective dose. For the main operator, the average increase was 43% while for the assistant operator, the increase was 32%. Increasing the exposed body surface leads to an increase in the diffusing volume and subsequently the dose of the operators. This logic is accentuated when the X-ray tube voltage is raised (Compton effect), hence the need for optimal beam collimation.

### 3.1.3 Operator position effect

During the examination period, several workers may be present in the intervention room and are exposed to radiation, hence dosimetric monitoring to optimize staff positioning is needed [24]. In this study, the ( $E/KAP$ ) quantity for 10 locations was calculated for the second scenario (see Figure 3) to achieve this goal.

According to Figure 5, the sixth position appears to be the most irradiated position due to its proximity to both the X-ray tube and the patient who is considered the center of scattered radiation (both primary and scattered radiation are shifted to the left side of the patient: heart side). By comparing the distances separating the operators and the X-ray source, we find that, the closer the operators are standing to the radiation beam, the higher is their effective dose. This is demonstrated by the following comparison:

- Dose:  $D_6 > D_2 > D_5 > D_1 > D_7 > D_3 > D_8 > D_4 > D_9$
- Distance (operator - X ray tube):  $d_6 < d_2 < d_5 < d_1 < d_7 < d_3 < d_8 < d_4 < d_9$

In principle, the 2<sup>nd</sup> and the 6<sup>th</sup> positions should receive the same scattered radiation. However, they receive different doses since the beam axis is nearer to the 6<sup>th</sup> position given the position of the patient's heart and the 2<sup>nd</sup> position is shielded by the lead table side shield.

The 10<sup>th</sup> position violates the radiation beam proximity tendency of increased dose. Although it is closer than the 4<sup>th</sup>, 8<sup>th</sup> and 9<sup>th</sup> positions relative to the radiation beam center, it scored the lowest dose since the operator in this case is partially shielded by the C-arm machine that plays the role of a barrier.

Based on this dosimetric monitoring, the estimated dose of each position can be used to describe the different locations that can be occupied by operators

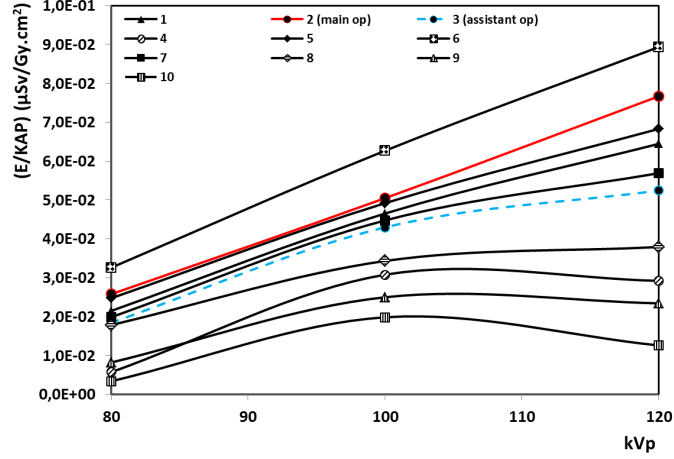


Figure 5. Effective dose  $E/KAP$  as a function of kVp for different operator positions during an interventional cardiology procedure.

during interventional procedure:

- The 2<sup>nd</sup> and 6<sup>th</sup> positions are the most irradiated as they are the closest to the primary and scattered radiation center. These are the positions where the main operators (cardiologists) who are primarily responsible for the intervention would most probably be standing.
- The 1<sup>st</sup>, 3<sup>rd</sup>, 5<sup>th</sup> and 7<sup>th</sup> positions have a lower dose than the first group. These positions are usually occupied by assistants and trainees who's role is secondary in the intervention procedure.
- The remaining positions 4<sup>th</sup>, 8<sup>th</sup>, 9<sup>th</sup> and 10<sup>th</sup> are the least irradiated positions as they are the most distant from the primary and scattered radiation centers. They can be occupied by radiological technicians, nurses or anesthesia technicians.

It should be noted that all the positions studied (except those occupied by the main operator: 2 and 6) are not constantly occupied during the intervention. The secondary actors (assistants, nurses, etc.) according to their task can move in and out the room, which results in a significant reduction of the dose. This condition was not considered in this study where we chose to assess the extreme cases of exposure with the highest doses.

#### 3.1.4 Projection modality effect

In this part, we will study the influence of the type of the chosen projection on the dose received by the male main operator during the third scenario.

We notice from the Figure 6, that the  $E/KAP$  coefficients by the AP projec-

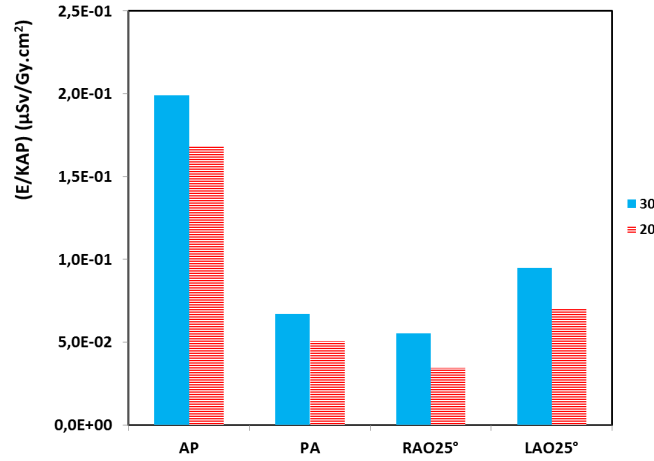


Figure 6. Effective dose ( $E/KAP$ ) for the main male operator for different projection modalities and FOV (during the third scenario: 100  $kVp$ ).

tion are almost three times higher than those by the other projections. Compared to the cases where the tube is located below the table (PA) and at the oblique planes ( $LAO25^\circ$  and  $RAO25^\circ$ ), the AP projection mainly allows an increase in the  $H_T/KAP$  coefficients at the eye lens, thyroid and brain by a factor of 1.43, 2.96 and 2.85 respectively (Figure 7). Therefore, doses of unprotected parts of the body like the brain must be monitored by optimizing the most appropriate projection.

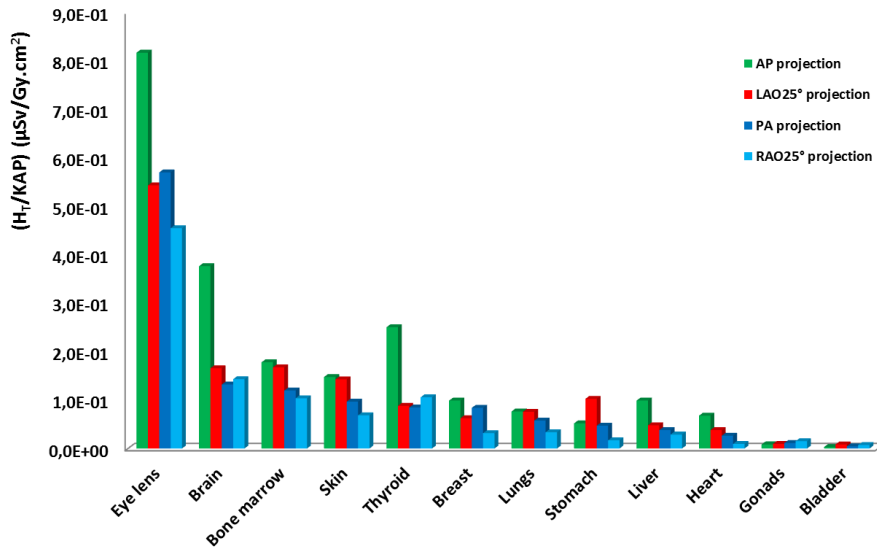


Figure 7. Equivalent dose ( $H_T/KAP$ ) for some organs for the main male operator for different projection modalities ( $kVp = 100$   $kVp$ ,  $FOV = 20 \times 20$   $cm^2$ ).

Therefore, it is recommended that the X-ray tube is placed under the patient's table whenever possible. In this case, the scattered radiation will be directed away from the head and more towards the lower body of the main operator.

The  $LAO25^\circ$  projection becomes the most critical projection for the main operator compared to the other two projections PA and  $RAO25^\circ$  because of their position relative to the primary and the scattered radiation centers. So, it would be better for the operator to stand in front of the X-ray tube than to its side since they will be shielded by the patient's body and minimally exposed.

The comparison between  $H_T/KAP_{Female}$  and  $H_T/KAP_{Male}$  for  $RAO25^\circ$  projection (kVp= 100 kVp, FOV=  $20 \times 20 \text{ cm}^2$ ) shows that the equivalent doses calculated for the main female operator is slightly higher than those of her male counterpart (Figure 8). The only explanation for these deviations is the difference in geometric shape and weight of the organs between the two sexes (the woman's organs weigh less than those of the man except breast tissue) which is confirmed by the discussion included in the ICRP Publication [26]. The difference between the effective dose for male ( $E/KAP_{Male}$ ) and female ( $E/KAP_{Female}$ ) operators worths 14.17 % for  $RAO25^\circ$  projection.

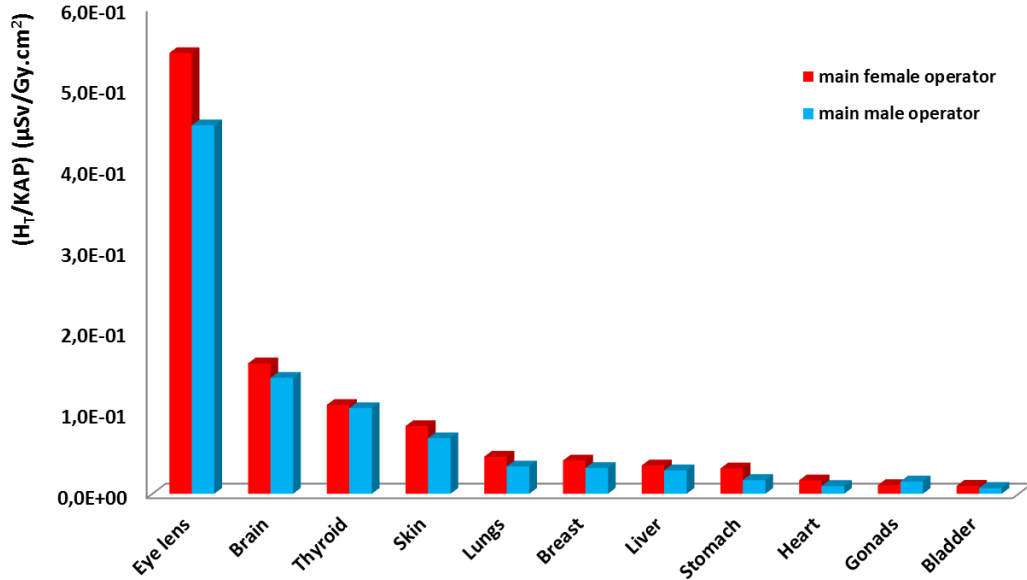


Figure 8. Comparison of equivalent dose ( $H_T/KAP$ ) for some organs of the main male and female operators, for  $RAO25^\circ$  projection (kVp= 100 kVp, FOV=  $20 \times 20 \text{ cm}^2$ ).

### 3.2 Dosimetric evaluation for the patient

This part studies the influence of some parameters on the patient dose undergoing cardiac intervention procedure.

### 3.2.1 Comparison between $(E/KAP)_{Male}$ and $(E/KAP)_{Female}$

The  $E/KAP$  coefficient for both male and female phantoms was calculated for the scenarios 4.1 and 4.2 respectively.

We notice from the Figure 9 that the  $E/KAP$  ( $mSv/Gy.cm^2$ ) for the patient increases with the increase of the tube voltage and the field size. This is expected because, the increase of the  $E/KAP$  coefficient is induced by the increasing energy of the beam. The KAP value, given by the absorbed dose in air, reaches a maximum around 60 keV beyond which it starts to decrease with the increasing beam energy, therefore resulting in a higher  $E/KAP$ .

Nevertheless, it is important to note that the results were obtained without taking into account the automatic exposure control that is usually functioning in this kind of equipment.

In addition, a comparison between  $(E/KAP)_{Female}$  and  $(E/KAP)_{Male}$  shows that the woman always scored higher values for the three studied projections than those of the male patient. The average differences vary from 6.6 % for the PA projection to 33 % for  $RAO25^\circ$  projection. So, without consideration of the automatic adjustment of the exposure parameters usually applied in real operations where the body mass index varies from one patient to another, we conclude that body size and habitus have an effect on the effective dose of the patient, which in turn can directly affect the energy deposition and radiation transport.

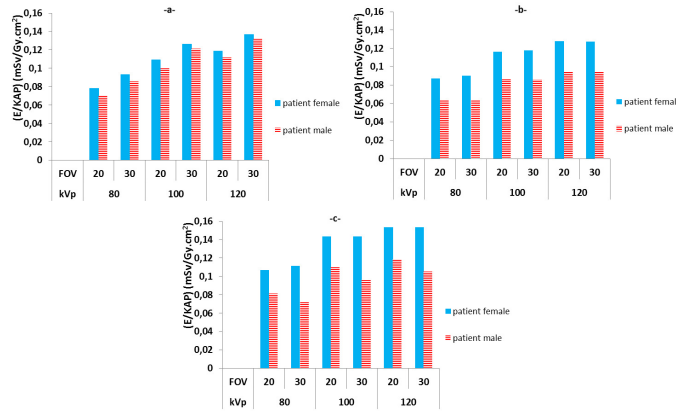


Figure 9. Effective dose for male and female patients as a function of kVp and FOV: (a) Postero-Anterior ( $PA$ ), (b) Right Anterior Oblique ( $RAO25^\circ$ ) and (c) Left Anterior Oblique ( $LAO25^\circ$ ).

### 3.2.2 Projection modality effect

To assess the influence of the type of projection chosen ( $AP$  /  $PA$  /  $LAO25^\circ$  /  $RAO25^\circ$ ), the  $E/KAP$  and the  $H_T/KAP$  were calculated for the main radiosensitive organs of a male patient during the third scenario. These results

are depicted in the following figures 10 and 11.

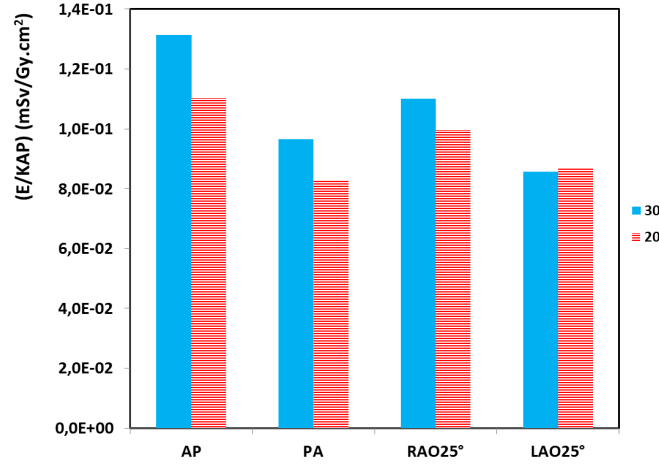


Figure 10. Effective dose ( $E/KAP$ ) for the male patient for different projection modalities and FOV (during the third scenario: 100  $kVp$ ).

As shown in Figure 10, the highest  $E/KAP$  values were obtained for the  $AP$  projection due to the direct exposure of the patient by the X-ray beam, while the values of the three other projections  $PA$ ,  $LAO25^\circ$  and  $RAO25^\circ$  are lower than those of the  $AP$  projection. This dose reduction is attributed to the most radiosensitive organs are closer to anterior surface and they are protected by the spine and posterior musculature, therefore, in the  $PA$  projection they are further away from the beam entrance surface compared to an  $AP$  projection, and to the tissue compression (the patient abdominal diameter decreases by switching to a  $PA/LAO25^\circ/RAO25^\circ$  projection).

Consequently, it is recommended that the X-ray tube is located under the table allowing a significant reduction in the patient dose by an average factor of 1.34.

Given that the  $AP$  projection is not recommended in the clinical procedures, the  $RAO25^\circ$  projection becomes the most critical situation for the patient compared to the other two projections  $PA$  and  $LAO25^\circ$  during the interventional cardiology procedures.

As expected, organs located inside or near the radiation field such as the heart and lungs have higher  $H_T/KAP$  of the order of  $mSv/Gy.cm^2$  while the organs distant from the area of interest have lower values, tending to be zero (Figure 11).

Organs positioned asymmetrically, like the heart (located on the left side of the patient) had higher values of  $H_T/KAP$  for  $RAO25^\circ$  projection. On the other hand, the liver (located on the right side of the patient) had higher values  $H_T/KAP$  for  $LAO25^\circ$  projection.



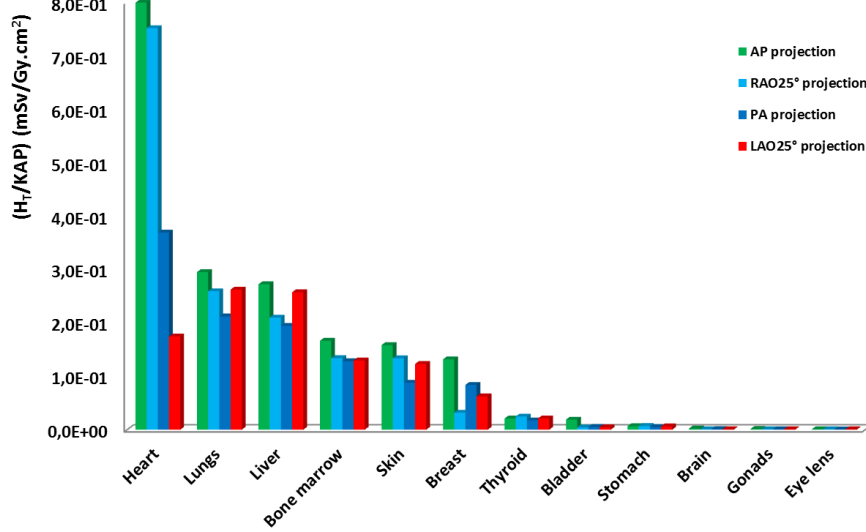


Figure 11. Equivalent dose ( $H_T/KAP$ ) for some organs for the male patient for different projection modalities ( $kVp=100\text{ kVp}$ ,  $FOV=20 \times 20\text{ cm}^2$ ).

In this assessment, we must take into account an important point. In real context, only a well-defined part of the skin is directly irradiated, counter to our simulation the  $H_T/KAP$  to the skin concerns the entire body of the patient. Therefore, it is advisable to use our calculated coefficients only for the estimation of effective doses.

From the Figure 12, it was again confirmed that an increase in the tube voltage, from 80 to 120  $kVp$ , leads to an increase in the  $E/KAP$  for both the patient and the main operator. The scattering radiation from the patient increases with increasing  $kVp$ , thus leading to an increase in the  $E/KAP$  to the medical staff. According to this correlation between the doses of patients and staff, we can affirm that the radiation protection of the patient and the professional are interdependent. So, reducing the patient's dose also reduces the operator's dose.

### 3.3 Comparison with previous work in the literature

Our results are based on MC simulations, and validation with experimental data is very important. That is why, we resorted to compare our results with those from the literature (simulated and experimental data). The average  $E/KAP$  coefficient (per scenario) was determined for the patient and the main operator during the fourth scenario with the two sub-scenarios (for all projections and tube voltages, and for  $20 \times 20\text{ cm}^2$  of FOV).

According to Table 3, the average  $E/KAP$  coefficient for the patient was estimated by  $3.05 \times 10^{-1}\text{ mSv/Gy.cm}^2$  which is in moderate agreement with the

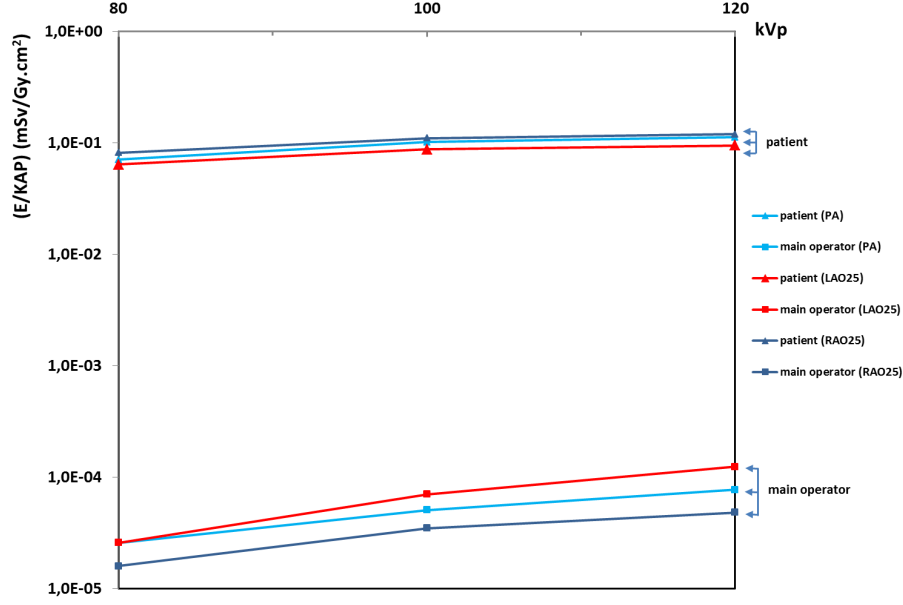


Figure 12. Correlation between patient and medical staff effective doses in interventional cardiology procedures.

<i>E/KAP (mSv/Gy.cm<sup>2</sup>): Patient</i>					
Efstathopoulos <i>et al.</i> [27]	Bor <i>et al.</i> [28]	Santos <i>et al.</i> [4]		Our work	
		M90-H90 phantom	M10-H10 phantom		
1.80×10 <sup>−1</sup>	2.40×10 <sup>−1</sup>	1.90×10 <sup>−1</sup>	3.50×10 <sup>−1</sup>	3.05×10 <sup>−1</sup> (± 0.2%)	
<i>E/KAP (μSv/Gy.cm<sup>2</sup>): Main operator</i>					
Tsapaki <i>et al.</i> [29]	Ferrari <i>et al.</i> [3]	Bor <i>et al.</i> [28]	Santos <i>et al.</i> [4]		Our work
			M90-H90 phantom	M10-H10 phantom	
1.32×10 <sup>−1</sup> -1.68×10 <sup>−1</sup>	1.77×10 <sup>−1</sup>	1.40×10 <sup>−1</sup>	1.90×10 <sup>−1</sup>	1.30×10 <sup>−1</sup>	1.65×10 <sup>−1</sup> (± 2%)

Table 3

Comparison of our results with those of previous works in the literature.

simulated results reported by Santos *et al.* [4] in the range of  $1.90 \times 10^{-1}$  –  $3.50 \times 10^{-1}$   $mSv/Gy.cm^2$  depending on the used phantom and its body mass index. Also, we found that our values are not too far from those recorded by the experimental work of Efstathopoulos *et al.* [27] and Bor *et al.* [28] during cardiac intervention procedures.

Similarly for the main operator, in our work the  $E/KAP$  was estimated by  $1.65 \times 10^{-1} \mu Sv/Gy.cm^2$  which is in good agreement with the simulated results reported by Ferrari *et al.* [3] and Santos *et al.* [4]. A good correspondence is also underlined with each of the following experimental results: the work of Tsapaki *et al.* [29] reported an  $E/KAP$  coefficient of  $1.32 \times 10^{-1} \mu Sv/Gy.cm^2$  for angiography procedures and  $1.68 \times 10^{-1} \mu Sv/Gy.cm^2$  for coronary angioplasty, and the work of Bor *et al.* [30] for coronary angiography procedures which confirms our estimates.

Our results are within the expected values and are in agreement with the work of previous teams. The small variations from the experiments and simulations are due to the differences in equipment, phantom types, simulation codes and statistical errors.

This proves the validation of this present work in dose estimation for patients as well as medical staff in interventional cardiology procedures. And this efficiency has consequently enabled to deepen the study in the following part.

### 3.4 Influence of radiation protection equipment on exposed operators

It has been proven that interventional cardiology procedure is often associated with an elevated occupational radiation exposure, hence the need for good dosimetric monitoring and the employment of the appropriate radiation protection equipment. In common practice and apart from theoretical considerations, several cases of operators with immediate or long-term undesirable effects are revealed despite the use of personal protective equipment (PPE) such as lead aprons, thyroid shields or mobile screens which protect only the covered area. Therefore, the risk was underlined for the head and lower and upper extremities which are generally deprived of protection [31].

In addition, the regular use of PPE can cause orthopaedic pathologies in the long term in particular due to the weight of the lead apron (between 4 kg and 8 kg) used during long and complex cardiology procedures.

In this section, we evaluate the effectiveness of a new means of protection: the mobile radiation protection cabin, carried out during our fifth scenario. Following the implementation of the radiation protection cabin, we can notice from the values reported in Table 4 a significant decrease in doses at the level of all the organs of the both male and female main operators. This reduction can reach an average of 83.88 %.

On the other hand, when comparing with the results of other personal protective equipment used in our scenarios 1-4 (lead apron+ thyroid shield+ eye glasses) and in previous work (lead apron) [4], we find that RPC provides at least the same radiation protection rate as a routine protection equipment in addition to providing a cover to almost the entire body of the medical staff. This validates the almost total radiation protection effectiveness of this cabin

in the main operator's case, as well as the comfort while performing his task. Therefore, this innovative radioprotective device is a good alternative that can be used by interventional cardiologists, in particular young female cardiologists and experienced ones who have accumulated exposure over time.

		Previous work [4]	Our work			
means of protection		lead apron	Routine equipment		RPC	
Organ \ Gender		male	male	female	male	female
	Eye lens	-	66.15	65.91	77.19	77.32
	Brain	-	11.81	11.21	81.4	81.28
	Breast	95	88.13	88.79	89.19	89.78
	Skin	-	42.1	42.16	76.14	76.21
	Thyroid	-	69.87	68.11	80.18	80.13
	Lungs	89	83.12	83.61	90.19	90.31
	Stomach	90	81.7	83.12	79.15	78.2
	Liver	91	81.61	81.15	88.98	88.71
	Heart	-	80.76	80.19	86.15	86.51
	Testes	81	83.08	-	82.19	-
	Uterus	-	-	80.61	-	89.12
	Bladder	-	83.1	82.88	90.88	90.2

Table 4

Comparison of percentage reduction in equivalent dose  $H_T/KAP$  for some organs of the main male/female operators when using routine equipment and radiation protection cabin. Exposure parameters in all cases: PA projection, kVp= 120 kVp, FOV=  $30 \times 30 \text{ cm}^2$ .

It is worthy to mention that wearing lead aprons remains compulsory for other staff given that the RPC is designed to protect only one operator who is the most exposed.

The current study proposes limitations to interventional practice. Computation time reduction of MC simulations would be beneficial for real-time dosimetric estimates. In addition, patient dose reduction should be investigated by employing a specialized cabin adjustable according to the specificity of the intervention.

Finally, this work is not limited to cardiac intervention and could be extended to investigate other types of medical radiation procedures. The proposed simulation can also be integrated for medical imaging purposes in addition to dosimetry and radiation protection.

## 4 Conclusion

The present work was motivated by the limited dosimetric monitoring in the literature for interventional cardiology procedures which often involve high X-ray radiation doses to the patients and the medical staff. The principal operator usually performs several cardiac intervention procedures per day and this exposes them to the accumulation of radiation doses especially since they stand closest to both the patient and the X-ray source. We can deduce from this study that following a certain protocol will considerably reduce the effective dose especially for sensitive organs of the main operator. Moreover, applying a good collimation better directs the beam away from the operators thus reducing the dose. Other medical staff are usually less exposed because the nature of their tasks does not oblige them to stand as close to the patient and in principle they accumulate less dose. In addition, a considerable reduction in dose was noticed when using radiation protection cabin. This reduction can reach an average of 83.88 %, motivating further investigation and perhaps the upgrading of personal protection equipment effectiveness in such interventions.

GEANT4 Monte Carlo code was used in this study to assess the risk of several radiation exposure situations in interventional cardiology by calculating conversion factors connecting radiation protection quantities with exposure index ( $E/KAP$ ) to evaluate the human carcinogenic risk ( $H_T/KAP$ ). Two radiation protection quantities  $E$  and  $H_T$  for critical organs/tissues were calculated and normalized by  $KAP$  values for both the patient and the operator. We evaluated the average  $E/KAP$  for the patient:  $3.05 \times 10^{-1} \text{ mSv/Gy.cm}^2$  and for the main male operator:  $1.65 \times 10^{-1} \text{ } \mu\text{Sv/Gy.cm}^2$ . These results are within the expected values and are in good agreement with those of previous works from the literature .

The calculated quantities were closely dependent on the X-ray beam quality ( $kVp$ ) and to a lesser extent on the radiation field size ( $FOV$ ) as well as the used projection modality. The medical staff organ dose was highly dependent on the staff location with respect to the beam source and the patient which was a major interest of this study.

Although using voxelized *ICRP110* computational reference phantoms enables the detailed calculation of effective doses in all sensitive organs and tissues, it remains a lengthy procedure given the computational requirements of Monte Carlo simulations. Although indicative, these phantoms are not case specific where differences in body mass index, weight, height and consequently organ sizes, from one person to another is not taken into consideration. Nevertheless, this dosimetric study could possibly be applied to any other interventional procedure with the possibility to develop a dose calculation software based on the data extracted from the simulations not to mention the future prospect of delivering a dedicated *GEANT4* example for manipulating the voxelized phantoms and organ dose assessment.

## References

- [1] Vañó E, González L, Guibelalde E, Fernández JM, Ten JJ. Radiation exposure to medical staff in interventional and cardiac radiology. *Br J Radiol* 1998;71(849):954–60.
- [2] Brambilla M, Cannillo B, Guzzardi G, et al. Conversion factors for effective dose and organ doses with the air kerma area product in patients undergoing percutaneous transhepatic biliary drainage and trans arterial chemoembolization. *Phys Medica* 2020; 72: 7-15.
- [3] Ferrari P, Becker F, Jovanovic Z, Khan S, Bakhanova E, Principi S, et al. Simulation of H p (10) and effective dose received by the medical staff in interventional radiology procedures. *J. Radiat. Prot. Res.* 2019;39(3):809.
- [4] Santos WS, Belinato W, Perini AP, Caldas LV, Galeano DC, Santos CJ, Neves LP. Occupational exposures during abdominal fluoroscopically guided interventional procedures for different patient sizes—A Monte Carlo approach. *Phys Medica* 2018;45:35-43.
- [5] Cavalcante FR, Junior AC, Santos WS, et al. Monte Carlo simulation of interventional cardiac scenarios using a newborn hybrid phantom and MCNPX code. In *World Congress on Medical Physics and Biomedical Engineering*, June 7-12, 2015, Toronto, Canada (pp. 173-176). Springer, Cham.
- [6] Schultz F W, Zoetelief J. Dosemeter readings and effective dose to the cardiologist with protective clothing in a simulated interventional procedure. *Radiat Prot Dos* 2008 ;129(1-3): 311-315.
- [7] Goorly JT, James MR, Booth TE, et al. Initial MCNP6 release overview-MCNP6 version 1.0(2013).
- [8] Emfietzoglou D, Bousis C, Hindorf C, et al. A Monte Carlo study of energy deposition at the sub-cellular level for application to targeted radionuclide therapy with low-energy electron emitters. *Nucl. Instrum. Methods Phys. Res. B* 2007 ;256(1):547-553.
- [9] Baro J, Sempau J, Fernández-Varea J M, et al. *PENELOPE*: an algo-

- rithm for Monte Carlo simulation of the penetration and energy loss of electrons and positrons in matter. Nucl. Instrum. Methods Phys. Res. B 1995 ; 100(1): 31-46.
- [10] Kawrakow I. Accurate condensed history Monte Carlo simulation of electron transport. I. EGSnrc, the new EGS4 version. Med Phys 2000 ; 27(3): 485-498.
  - [11] Ghal-Eh N, Goudarzi H, Rahmani F. FLUKA simulation studies on in-phantom dosimetric parameters of a LINAC-based BNCT. Radiat Phys Chem 2017; 141:36-40.
  - [12] Elhamdi K, Manai K, Bhar M. Dose calculation using Tchebyshev wavelets with buildup correction in the Tunisian gamma irradiator. Radiat Phys Chem 2018 ;150: 46-50.
  - [13] Bhar M, Kadri O, Manai K. Assessment of self-and cross-absorbed SAF values for HDRK-man using Geant 4 code: internal photon and electron emitters. Nucl Sci Tech 2019; 30(10):149.
  - [14] Ounalli L, Bhar M, Mejri A, et al. Combining Monte Carlo simulations and dosimetry measurements for process control in the Tunisian Cobalt-60 irradiator after three half lives of the source. Nucl Sci Tech 2017 ;28(9): 133.
  - [15] Belkadhi K, Elhamdi K, Bhar M, Manai K. Dose calculation using Haar wavelets with buildup correction. Appl. Radiat. Isot 2017;127:186-194.
  - [16] Papadimitroulas P. Dosimetry applications in GATE Monte Carlo toolkit. Phys Medica 2017; 41:136-140.
  - [17] International Commission on Radiological Protection. Adult reference computational phantoms. ICRP Publication 110. Oxford: Elsevier 2009.
  - [18] Agostinelli S, Allison J, Amako KA, et al. GEANT4—a simulation toolkit. Nucl Instrum Methods Phys Res A 2003; 506(3): 250-303.
  - [19] Allison J, Amako K, Apostolakis J, et al. Recent developments in Geant4. Nucl Instrum Methods Phys Res A 2016 ; 835 :186-225.
  - [20] Allison J, Amako K, Apostolakis J E A, et al. Geant4 developments and applications. IEEE Trans Nucl Sci 2006 ; 53(1) :270-27.
  - [21] Incerti S, Seznec H, Simon M, Barberet P, Habchi C, Moretto P. Monte Carlo dosimetry for targeted irradiation of individual cells using a microbeam facility. Radiat Prot Dosim 2009; 133(1):2-11.
  - [22] Allison J, Asai M, Barrand G, , et al. The geant4 visualisation system. Computer Physics Communications 2008; 178(5): 331-365.
  - [23] Poludniowski G, Landry G, DeBlois F, Evans PM, Verhaegen F. SpekCalc: a program to calculate photon spectra from tungsten anode x-ray tubes. Phys. Med. Biol 2009; 54(19):433.
  - [24] Efstathopoulos EP, Pantos I, Andreou M, et al. Occupational radiation doses to the extremities and the eyes in interventional radiology and cardiology procedures. Brit J Radiol 2011; 84(997): 70-77.
  - [25] ICRP Publication 103. The 2007 recommendations of the international commission on radiological protection. Ann 2007;37(24).
  - [26] ICRP, Conversion coefficients for radiological protection quantities for

- external radiation exposures, ICRP publication 116, Ann. ICRP 40 (2e5) (2010).
- [27] Efsthathopoulos EP, Makrygiannis SS, Kottou S, Karvouni E, Giazitzoglou E, Korovesis S, et al. Medical personnel and patient dosimetry during coronary angiography and intervention. *Phys Med Biol* 2003;48:3059–68.
  - [28] Bor D, Sancak T, Olgar T, Elcim Y, Adanali A, Sanlidelk U, Ak-yar S. Comparasion of effective doses obtained from dose area product and air kerma measurements in interventional radiology. *Br J Radiol* 2004;77:315–22.
  - [29] Tsapaki V, Kottou S, Patsilinakos S, Voudris V, Cokkinos DV. Radiation dose measurements to the interventional cardiologist using an electronic personal dosimeter. *Radiat Prot Dosim* 2004;112:245–9.
  - [30] Bor D, Onal E, Olgar T, Caglan A, Toklu T. Measurement and estimation of cardiologist dose received in interventional examinations. AAPM 48th annual meeting, Orlando, USA. 2006. pp. 1–1.
  - [31] Dragusin O, Weerasooriya R, Jaïs P, Hocini M, Ector J, Takahashi Y, et al. Evaluation of a radiation protection cabin for invasive electrophysiological procedures. *Eur Heart J* 2007; 28(2):183-189.